Journal of Drug Delivery Science and Technology 61 (2021) 102242

Contents lists available at ScienceDirect

Journal of Drug Delivery Science and Technology

journal homepage: www.elsevier.com/locate/jddst

Research paper

Intranasal delivery of chitosan decorated PLGA core /shell nanoparticles containing flavonoid to reduce oxidative stress in the treatment of Alzheimer's disease

Namdev Dhas, Tejal Mehta *

Institute of Pharmacy, Nirma University, Ahmedabad, Gujarat, 382481, India

ARTICLE INFO

Keywords:
Curcumin
Core/shell nanoparticles
Antioxidant activity
BBB co-Culture model
Systemic toxicity

ABSTRACT

Curcumin (Cur), an antioxidant flavonoid has demonstrated high efficiency in attenuating oxidative stress in Alzheimer's disease (AD). Nevertheless, despite of its therapeutic potential, its clinical applications are hindered due to low solubility and low bioavailability and and first-pass metabolism. Thus, we fabricated Cur encapsulated chitosan functionalized PLGA core/shell NPs (CH@Cur-PLGA C/S NPs) and administered via intranasal route. Research also include comparative study of PLGA NPs (core) and CH@Cur-PLGA C/S NPs (C/S NPs) to investigate effect of CH coating over PLGA NPs on therapeutic efficacy, cellular uptake and stability. Fabricated NPs were extensively characterized and confirmed Cur encapsulation with 75% of entrapment efficiency and particle size in the range of 200 nm. TEM analysis confirmed uniform coating of CH over PLGA NPs. Release and permeation study demonstrated sustained release and enhanced permeation through nasal mucosa. Cellular uptake mechanism showed caveolae-mediated-enhance endocytosis of NPs. *In-vitro* BBB-co-cufure model exhibited efficient passage for C/SNPs. Antioxidant assay demonstrated significant ROS scavenging activity of C/SNPs. *In-vivo* toxicity showed insignificant toxicity. Bio-distribution of C/S NPs was higher in brain following intranasal route. Photo and thermal stability confirmed protection of Cur by C/SNPs. Obtained results demonstrate potential application of C/SNPs for reducing oxidative stress in brain for effective AD treat.

1. Introduction

Alzheimer's Disease (AD) is progressive neurodegenerative disease characterized by elevated oxidative stress, neuronal and synapses loss, deposition of Aβ plaques and neurofibrillary tangles and many more. Currently, the US-FDA-approved medications for AD treatment are N-methyl-D-aspartate (NMDA) receptor and acetylcholineesterase (AchE) inhibitors, however, these medications will only alleviate the symptoms of AD marginally [1]. As mentioned above, oxidative being one of the cause of AD, the drug with antioxidant activity can be a good candidate for AD treatment. In this case, many flavonoids with antioxidant activity have been explored for treating AD.

Cur, a hydrophobic natural polyphenol compound derived from rhizomes of *Curcuma longa*, possibly a multi-purpose drug owing to its widespread applicability in Alzheimer's disease, Parkinson's disease, prophylaxis, pro-inflammatory chronic disease, cancer including multiple sclerosis, atherosclerosis, pulmonary diseases and many more. However, the medical applications of Cur have been limited due to its low solubility, rapid metabolism and bioavailability. Undeniably, Cur has an extremely low solubility at different pH ranges viz. 11 ng/ml in aqueous buffer at pH 5, 0.0004 mg/ml at pH 7.4. Furthermore, under physiological conditions, Cur undergoes a rapid hydrolysis, being degraded with major product trans-6-(4-hydroxy-3-methoxyphenyl)-24-dioxo-5-hexenal and minor degradation product viz. ferulic acid, feruloyl methane and vanillin. Cur is also susceptible to photodegradation that could be problematic for long-term storage [2].

Thus, fabrication of nanoparticles (NPs) for the transport of drugs to the brain for AD in the last few decades has promised an increasing interest in solving several disadvantages of conventional therapy viz. non-specificity towards target site, poor blood brain barrier (BBB) permeation, systemic and healthy cell toxicity. NPs-based delivery carriers have attracted much attention from researchers due to its various merits viz. solubility enhancement, dose reduction, dose frequency reduction and enhance brain targeting efficiency via intranasal pathway.

Intranasal pathway is used to enable administration of therapeutic

* Corresponding author.
E-mail address: tjshah3@gmail.com (T. Mehta).

https://doi.org/10.1016/j.jddst.2020.102242
Received 24 May 2020; Received in revised form 18 November 2020; Accepted 19 November 2020
Available online 24 November 2020
1773-2247/

moiety avoid hepatic and gastrointestinal metabolism. Nasal mucosa possesses a large surface area and high vascularization owing to which it provides enhancement in drug absorption followed by increase in therapeutic effect initiation. Nevertheless, there are certain demerits of nasal delivery for example, due to mucociliary clearance there can be rapid removal of the drug/carrier from the absorption site leading to less absorption hampering therapeutic effect [3].

Core Shell NPs (C/S NPs) showed great potential for use as delivery platform for nose to brain targeting of drugs, as they are biocompatible, biodegradable, manufacturing procedure is easy [4]. C/S NPs can effectively protect drug against P-gp efflux and external environmental degradation resulting into higher drug concentration at target site, as compared to simple NPs. C/S NPs exhibit great stability, tunable and sustained drug release when compared with simple NPs [5].

The study included PLGA as a core material owing to its biocompatible, biodegradable and non-toxic nature. It has high drug loading capacity and can be easily functionalized over the surface with other materials [6,7]. The second polymer included in the study was chitosan (CH), a cationic mucoadhesive polymer which will help in enhancing residence time at the site of action as positive charge of CH will interact electrostatically with negatively charged mucin also has the ability to form gel by absorbing water [8]. It has been reported that CH helps in opening tight junctions and enhances the permeation of drug through nasal mucosa. Thus CH could be a good candidate as shell material to increase residence time and improve drug permeation [9].

The current study portrayed the development of Cur encapsulated CH functionalized PLGA C/S NPs (CH@Cur-PLGA C/S NPs) for attenuating oxidative stress in AD using intranasal route. The study also aims at improving bioavailability and antioxidant activity of Cur along with stability and reduction in toxicity. CH@Cur-PLGA C/S NPs was developed using nanoprecipitation method followed by electrostatic interaction to coat CH (shell) over PLGA NPs (core). The optimized NPs were extensively characterized and were further evaluated using various *in-vitro* techniques, and cell line studies viz. *in-vitro*-cytotoxicity, cellular uptake, cellular uptake mechanism, ROS generation study and BBB passage study. *In-vivo* bio-distribution of NPs in various organs was determined after intranasal administration and was performed by conjugating FITC on the surface of NPs. All the aforementioned study was performed in comparative way within pure Cur, placebo PLGA NPs, Cur loaded PLGA NPs (Cur-PLGA NPs), placebo CH@PLGA C/S NPs) and CH@Cur-PLGA C/SNPs. The present research demonstrated the reduction in oxidative stress by use of flavonoid encapsulated C/SNPs following intranasal route.

2. Materials and methods

2.1. Materials and reagents

PLGA (50:50) (MW = 7–17 KDa) were received as a gift sample from Evonik Industries (Essen, Germany. Low molecular weight chitosan (50–190 KDa) with 75% deacetylation was purchased from Sigma-Aldrich (Bangalore, India). Chloroacetic acid, dialysis membrane (cut-off 12000 Da), Dulbecco's Modified Eagle Medium (F12 Ham DMEM/F12, 1:1 mixture), fetal bovine serum albumin, MTT, L-glutamine, penicillin, streptomycin, isopropyl alcohol, acetone, procured from Himedia (India). Sephadex G-50 was purchased from MPBiomed. All other chemicals were purchased of analytical grade. SHSY5Y human neuroblastoma, RPMI-2650, RAW 264.7, MDCK-II and U-373 MG cell lines were procured from NCCS, Pune, India.

2.2. Fabrication of placebo PLGA NPs and Cur-PLGA NPs

Nanoprecipitation method is one of the best techniques utilized for encapsulating hydrophobic drugs, thus utilized to fabricate Cur-PLGA NPs. Firstly, the blank PLGA NPs were fabricated using nanoprecipitation method as earlier stated by Dhas et al. with certain modifications [10]. Briefly, 5 mg/ml of PLGA was added in acetone to form organic phase, while 1% w/v pluronic-F127 was used to form aqueous phase. The PLGA solution was gradually added with a flow rate of 1 ml/min, into the aqueous solution with phase ratio of (1:6) (organic: aqueous) with the help of syringe and simultaneous magnetic stirring at 500 rpm. The colloidal solution was kept for stirring till the organic solvent is removed. Similarly, Cur-PLGA NPs was optimized following same procedure. 2 mg Cur was added along with PLGA into acetone to form organic phase. The encapsulated and un-entrapped Cur was separated by sephadex column (G-50). The obtained CUR-PLGA NPs were then lyophilized.

2.3. Preparation of CH@Cur-PLGA C/SNPs

The CH shell (positively charged NH_2-) was modified over PLGA NPs (negatively charged COOH-) using electrostatic interaction to form C/S NPs (CH@PLGA C/S NPs) [3,10]. Several concentrations of CH (0.01%, 0.02%, 0.03%, 0.04% w/v) was prepared and into it PLGA NPs and Cur-PLGA NPs colloidal solution added gradually in separated beakers. The stirring time and CH concentration was optimized using dependent variables such as particle size, surface charge and PDI. The prepared blank CH@PLGA C/S NPs and CH@Cur-PLGA C/S NPs were purified from un-reacted CH with the help of centrifugation at 10,000 rpm for 15 min. The prepared NPs viz. blank PLGA NPs, blank CH@PLGA C/SNPs, Cur-PLGA NPs and CH@Cur-PLGA C/SNPs were lyophilized using 5% mannitol (cryoprotectent) in lyophilizer at −70 °C.

2.4. Entrapment efficiency (EE) and drug loading (DL)

The colloidal solution of Cur-PLGA NPs and CH@Cur-PLGA NPs was passed through sephadex column blocking un-entrapped Cur in the column, which was further removed by adding Cur soluble solvent. Cur was estimated using UV-spectrophotometer at λ_{max} of 427 nm. The experiments were performed in triplicate. The %EE and %DL were determined using following equation.

$$\%EE = \frac{Amount\ of\ Cur\ in\ NPs}{Total\ amount\ of\ Cur\ added} * 100 \quad (1)$$

$$\%DL = \frac{Amount\ of\ Cur\ entrapped\ in\ NPs}{Total\ weight\ of\ formulation} * 100 \quad (2)$$

2.5. Characterization of prepared NPs

The prepared NPs viz. blank PLGA NPs, blank CH@PLGA C/SNPs, Cur-PLGA NPs, CH@Cur-PLGA C/SNPs and pure Cur, PLGA, CH were characterized for particle size, zeta potential, PDI, FTIR, pXRD and TEM. The particle size, zeta potential and polydispersivity was measured using zetasizer (Horiba). FT-IR spectra of prepared NPs homogenously mixed with KBr, was analysed in the wavenumber range of 400–4000 cm^{-1} using FTIR (FTIR spectrometer, IR Affinity- 1S (Shimadzu, Japan). pXRD patterns were analysed using X-ray diffractometer (Ultima IV, Rigaku) in the range of 5–50 (2θ value) to determine the degree of crystallinity. The morphology of the Cur-PLGA NPs and CH@Cur-PLGA C/S NPs was studied using Transmission electron microscopy ((TEM) (Philips-CM 200)). Briefly, 20 μl of Cur-PLGA NPs and CH@Cur-PLGA C/SNPs dispersion was put on copper grid coated with carbon film and air dried. Then phosphotungstic acid was added to stain Cur-PLGA NPs and CH@Cur-PLGA C/SNPs negatively and allow to stand for drying at room temperature, after that images were captured with magnification between 25× to 75000x.

2.6. In-vitro drug release profile

The release of Cur from Cur suspension, Cur-PLGA NPs and CH@Cur-PLGA C/S NPs was performed in phosphate buffer saline (pH 7.4)

containing 0.5% tween 80 (medium), using dialysis membrane diffusion method [11]. In brief, the 2 ml of CUR suspension and Cur-PLGA NPs and CH@Cur-PLGA C/S NPs colloidal solution with equivalent weight of Cur was added in dialysis membrane. The dialysis membrane further suspended in beaker containing 100 ml of medium. The system was maintained at 37±2 °C and stirring speed of 100 rpm. Aliquots were collected at predetermined time intervals from the medium outside the dialysis bag. The medium was immediately replaced with equal volume i.e. 0.5 ml of fresh phosphate buffer. The Cur concentration was measured using UV spectrophotometer at 427 nm. The experiment was performed in triplicate.

2.7. Ex-vivo diffusion profile

In order to examine the diffusion of Cur suspension, Cur-PLGA NPs and CH@Cur-PLGA C/S NPs across nasal mucosa, the *ex-vivo* diffusion study was carried out using franz-diffusion cell [11–13] Briefly, in between donor and acceptor compartment the nasal mucosa was fixed. Later, 2 ml of Cur suspension (2 mg/ml), Cur-PLGA NPs and CH@Cur-PLGA C/S NPs with equivalent weight of 4 mg of Cur in the NPs were added in the donor compartment individually. While, 25 ml of PBS containing 0.5% tween 80 was added in acceptor compartment. Aliquots were collected at predetermined time intervals from the acceptor compartment and were replaced with equal volume of freshly prepared PBS containing 0.5% tween 80. The Cur concentration was measured using UV spectrophotometer at 427 nm. The experiments were performed in triplicate.

2.8. In-vitro cell viability assay

The cytotoxic effect of prepared NPs (blank PLGA NPs, blank CH@PLGA C/SNPs, Cur-PLGA NPs, CH@Cur-PLGA C/SNPs) along with pure Cur was performed on RPMI 2650 and SH-SY-5Y cell lines using MTT assay [14]. In brief, cells were seeded on 96 well cell culture plates at a density of $1*10^4$ cells/well and left for seeding 24 h at 37 °C with 5% CO_2. The RPMI 2650 and SH-SY-5Y cells were separately exposed to distinct concentration i.e. 10–50 μg/ml of samples for 24 h. Further, the culture media was removed from each well plate and replaced with MTT solution with concentration of 5 mg/ml at 37 °C for 4 h. The medium was removed after incubation and then 150 μl of DMSO was utilized to dissolve formed formazan crystals, followed by absorbance of formazan reduction product using spectrophotometer at 570 nm using microplate reader (BioRad). The experiments were performed in triplicate.

2.9. Estimation of cellular uptake

The cellular uptake of FITC, FITC-blank PLGA NPs, FITC-blank CH@PLGA C/S NPs, FITC-Cur-PLGA NPs and FITC-CH@Cur-PLGA C/S NPs was quantitatively determined in SH-SY-5Y cell line using spectrofluorometer [15]. Briefly, the cells were seeded in 6-well plate at a density of $5*10^5$ cells/well and incubated for 24 h at 37 °C, under 5% CO_2 environment. The aforementioned samples with the concentration of 25 μg/ml were then incubated with cells, for 2 h at 37 °C and subsequently washed 3 times with the help of PBS. Later on, post-removal of the supernatant, cells were trypsinized and centrifuged for 5 min at 1500 rpm to obtain cell pellets. Further, cells were re-suspended in PBS followed by analysis using spectrofluorometer and the cellular uptake-related fluorescence intensity was measured.

2.10. Cellular uptake mechanism

Cellular uptake mechanisms of prepared NPs were determined using spectrofluorometer in SH-SY-5Y cell line. The cellular uptake of NPs can follow several endocytic pathways depending on the materials used to fabricate NPs, their surface charge and last but not the least size of NPs. Therefore, the investigation includes various endocytic inhibitors such as nystatin, chlorpromazine and sodium azide which inhibits caveolae-mediated pathway, clathrin-mediated pathway and macropinocytosis pathway [16]. Briefly, the cells were seeded on 6-well plate at density of $5*10^5$ cells/wells. Further, cells were pre-incubated for 1 h at 37 °C with different endocytic inhibitors at the following concentrations: chlorpromazine (10 μg/ml), nystatin (50 μg/ml) and sodium azide (0.1% w/v). After this pre-incubation, FITC-blank PLGA NPs, FITC-blank CH@PLGA C/SNPs, FITC-Cur-PLGA NPs and FITC-CH@Cur-PLGA C/SNPs were added and incubated for next 2 h. The cells were then washed three times with PBS followed by lysis of cells using Triton X-100 (1%) and analysed using spectrofluorometer. The cells when exposed to only individual NPs were considered as control and their uptake is designed as 100%.

2.11. Generation of ROS

RAW 264.7 cells were utilized to determine ROS generation when prepared NPs were exposed to cells [17]. The cells were seeded in 96 well-plate with the density of $2*10^4$ cells/well for 24 h. The samples viz. pure CUR, blank PLGA NPs, blank CH@PLGA C/SNPs, Cur-PLGA NPs, CH@Cur-PLGA C/SNPs were then added into the cells with distinct concentrations (10–50 μg/ml) in presence of 10 μg/ml of H_2O_2. The ROS was measured by incorporating 10 μM of H_2DCFDA to sample treated cells and observed signal generated from oxidized form (dichlorofluorescein; DCF) at 535 nm using microplate reader. The experiments were carried out in triplicate. The ROS generated was expressed as a ratio of the fluorescence of DCF of treated cells to that of untreated cells.

2.12. In-vitro BBB permeation study

In order to study the ability of NPs to cross BBB, in-vitro BBB permeation study was performed using in-vitro co-culture model of BBB [16]. Co-culture model was developed by seeding U-373 MG cells with density of $7.5*10^4$ cells per well on apical side of insert (Corning, New York) which was coated with gelatin solution (2% w/v) and permitted to grow for 30 min. The inserts were then placed into 12 well plates containing DMEM and incubated for 24 h at 37 °C. Further, the inner side of inserts were seeded with MDCKII cells with a density of $150*10^4$ cells/well and were incubated at 37 °C for 24 h. Later on, Cur-PLGA NPs and CH@Cur-PLGA C/S NPs along with pure Cur were diluted individually with serum free DMEM and were then added to luminal chamber of inserts at concentration of 1 ml/well (2 mg/ml). Later, withdrawal of 200 μl of medium at different time points i.e. 0, 2, 24, 48 h, was carried out from basal chamber. Equal amount of serum free DMEM was added into basal chamber to maintain sink condition. The permeation of pure Cur, Cur-PLGA NPs and CH@Cur-PLGA C/SNPs was measured using spectrofluorometer and transport ratio was calculated using formula,

$$transport\ ratio\ (\%) = \frac{Az}{A} * 100 \quad (3)$$

Where, Az indicates amount of Cur in basal chamber at zth h (2, 24, 48 h) and A indicates the amount of Cur added in apical chamber.

2.13. Evaluation of antioxidant enzyme activity

In order to determine the antioxidant activity of Cur-PLGA NPs and CH@Cur-PLGA C/S NPs along with pure Cur, the three different assays viz. superoxide dismutase (SOD), catalase (CAT) and monoldialdehyde (MDA) were performed using RAW 264.7 cell line. In brief, the cells were exposed to distinct concentrations (0 mM, 5 mM, 10 mM and 20 mM) of pure Cur, Cur-PLGA NPs and CH@Cur-PLGA C/S NPs for 20 h. The positive control group, pure Cur, Cur-PLGA NPs and CH@Cur-PLGA C/S NPs treated groups were then exposed to 500 μM of H2O2 for 8 h, respectively [18]. The SOD, CAT and MDA activity in cell was measured using a commercial kit (Sigma-Aldrich) according to the manufacturer's

instructions [18].

2.14. Bio-distribution study

All animal studies were approved, maintained, treated, housed and performed in accordance with the guideline of institutional animal ethical committee (Registration no. 883/PO/ReBi/S/05/CPCSEA and project no. IP/PCEU/PHD/24/2018/013).

In-vivo biodistribution of Cur-PLGA NPs and CH@Cur-PLGA C/SNPs along with pure Cur was carried out in male Sprague Dawley (SD) rats. Male Sprague Dawley (SD) rats with a weight ranging from 250 to 350 g were selected for *in-vivo* biodistribution study. SD rats were divided into 4 groups each consisting of 6 animals. Group I animals were administered with Cur suspension and group II received the Cur-PLGA NPs and group III received CH@Cur-PLGA C/SNPs (fluorescently labelled) equivalent to 4 mg/kg of Cur, respectively and group IV was considered as control. The method for biodistribution was followed which was previously reported with some modifications [19]. The tissues of control group were utilized for calibration curve when they were sacrificed. The standard curves were plotted distinctly for each tissues i.e. liver, kidney, lungs, brain, heart and spleen.

The 50 μl of formulation was instilled in each nostril of rats. Rats were held from the back in slanted position during intranasal administration. Briefly, rats were fixed in supine position and formulation was administered at nostrils by polyethylene 10 tube attached to microliter syringe. The formulation was pushed through the syringe gently for 5 min and allowed the rats to sniff the formulation slowly. Animals were sacrificed and different organs were isolated after predetermined time points (i.e. 12 and 24 h). The organs were homogenized using a tissue homogenizer with 5 ml of PBS and the homogenate was centrifuged at 15000 rpm for 30 min the supernatant was collected and filtered through 0.45 μm filter and analysed using spectroflurometer [16].

2.15. In-vivo toxicity studies

The prepared NPs were evaluated for in-vivo toxicity in mice in accordance with the standard guidelines [20]. This investigation includes three groups containing 6 mice/group. Group 1 (control)- Milli-Q water; Group 2: Cur-PLGA NPs; Group 3: CH@Cur-PLGA C/SNPs. The known amount of Cur-PLGA NPs and CH@Cur-PLGA C/SNPs (4 mg/kg equivalent body weight (mice) of Cur) (0.5 ml) was daily administered intranasally for seven consecutive days. Further, blood samples were collected for biochemical analysis by cardiac puncture and then animals were sacrificed humanely by administering sodium pentobarbital (60 mg/kg) intravenously. The liver was excised from all three groups, washed in ice cold PBS to remove superficial blood and stored at −80 °C for further study. Several haematological and biochemical parameters were measured to assess toxicity caused due to Cur-PLGA NPs and CH@Cur-PLGA C/SNPs.

2.16. Stability studies

2.16.1. Photo-stability study

The Cur has disadvantage of photo-degradation, thus need to study the ability of NPs to protect Cur when encapsulated within. The study was carried by exposing Cur suspension, Cur-PLGA NPs and CH@Cur-PLGA C/S NPs to UV light to UV-C 260 nm TUV T5 lamp (Philips, India) for 24 h [21]. In brief, the known amount of Cur and equivalent weight of Cur-PLGA NPs and CH@Cur-PLGA C/SNPs were dispersed in phosphate buffer (pH 7.4) containing 0.5% tween 80 and kept in different glass vials. Aliquots were collected at predetermine time interval of 4 h. The oxidation in the collected samples was avoided by adding BHT ethanolic solution (0.1% w/v). The samples were further treated with nitrogen and covered with aluminium foil for prevention of further oxidative losses [21]. Later, Cur was extracted and quantified using spectrofluorometer. The Cur stability was measured using following equation

$$stability\ of\ Cur\ (\%) = \frac{Ct}{C0} * 100 \quad (4)$$

Where, C_t and C_0 indicates Cur concentration at t time and initial time.

2.16.2. Thermal stability study

Similar to photo-stability, thermal stability of Cur and the ability of NPs to protect Cur from thermal effect was performed. In brief, pure Cur, Cur-PLGA NPs and CH@Cur-PLGA C/S NPs was dispersed in deionized water (1 mg/ml). The obtained colloidal solutions were filled in amber colour vials and exposed at 4 °C, 25 °C and 30 °C for 30 days. The samples were tested at 0, 7, 15 and 30 day (time interval) for particle size, PDI and surface charge [22].

2.17. Statistical analysis

All the results were analysed using the statistical software package Graph Pad Prism. All the experiments were performed thrice and were expressed as mean ± SD.

3. Result and discussion

3.1. Fabrication and optimization of prepared NPs

The placebo PLGA NPs and Cur-PLGA NPs were fabricated using nanoprecipitation method with slight modifications [10]. Blank CH@PLGA C/SNPs and blank CH@Cur-PLGA C/SNPs were fabricated by modifying CH over the surface of PLGA NPs via electrostatic interactions. The coating of shell was performed by varying CH concentration and stirring time and was optimized through particle size and zeta potential of CH@PLGA C/SNPs as per our previous report [10]. From obtained results, 0.01% w/v of CH concentration with 15 min of stirring time was selected as optimized values to achieve lower increment in size and PDI.

3.2. Characterization of prepared NPs

The average particle size, polydispersivity and surface charge of blank PLGA NPs and Cur-PLGA NPs was found to be 179.3 ± 2.34 nm and 193.2 ± 2.17 nm; 0.112 ± 0.009 and 0.124 ± 0.013; −28.5.10 ± 2.73 mV and −29.80 ± 1.21 mV, respectively. The encapsulation of Cur into PLGA NPs results into increase in size of NPs. Additionally, the Cur concentration also plays significant role and has positive effect on modulating dependent variables. The particle size and PDI of Cur-PLGA NPs increase with increase in Cur concentration in the formulation. The negative surface charge on PLGA NPs is owing to ionized carboxyl group in PLGA [10]. More negativity of surface charge indicates its stability. Similarly, the particle size, polydispersivity and surface charge of blank CH@PLGA C/S NPs was found to be.

The mean particle size, PDI and zeta potential of placebo CH@PLGA C/SNPs and CH@Cur-PLGA C/SNPs was found to be 190.7 ± 1.97 nm and 207.6 ± 2.71 nm; 0.153 ± 0.009 and 0.165 ± 0.075; +42.7.3 ± 2.29 mV and +31.9 ± 1.03 mV, respectively. The results indicated that particle size of blank CH@PLGA C/S NPs and CH@Cur-PLGA C/S NPs was increased when compared with blank PLGA NPs and Cur-PLGA NPs. This may be owing to the coating of CH over the surface of PLGA NPs [10]. The TEM analysis was carried out for further confirmation.

The entrapment of CUR in Cur-PLGA NPs and CH@Cur-PLGA C/S NPs was measured using sephadex column (G-50 (MP BioMed, Mumbai, India)). The colloidal solution of Cur-PLGA NPs and CH@Cur-PLGA NPs was passed through sephadex column blocking un-entrapped Cur in the column, which was further removed by adding Cur soluble solvent. Cur was estimated using UV-spectrophotometer at at λ_{max} of 427 nm. The % EE of optimized Cur-PLGA NPs and CH@Cur-PLGA C/S NPs was found

to be 79.12% ± 2.17% and 75.53% ± 2.09%, respectively; while %DL was found to be 5.01% ± 0.03%, 4.37 ± 0.09%, respectively.

The FTIR spectrums of pure Cur, CH, PLGA, blank PLGA NPs, blank CH@PLGA C/SNPs, Cur-PLGA NPs and CH@Cur-PLGA C/SNPs were shown in Fig. 1A. The PLGA showed characteristic peaks at 2972.31 cm^{-1} for C–H group, 1752 cm^{-1} for C═O stretching as well as 1082 cm^{-1} for C–O–C stretching [23]. The characteristic peak of CH at 1070.49 cm^{-1} is owing to C═O group stretching; 1517.98 cm^{-1} is assigned to the presence of stretching of free amino group; 1668.43 cm^{-1} is relative to the vibration of the carbonyl group of acetylated amide; 3469.72 cm^{-1} indicates that the O–H stretching overlapped with and N–H stretching vibration [24]. Pure Cur exhibited characteristic peaks at 1502.55 cm^{-1} representing C═O and C–C vibrations; 1600.92 cm^{-1} revealing stretching vibrations of benzene ring [25]. In case of blank PLGA NPs, all the characteristic peaks of PLGA were present. Blank CH@PLGA C/SNPs showed characteristic peaks of CH and PLGA indicating CH was coated over PLGA, also did not displayed any additional peak which indicates compatibility of both the polymers. Furthermore, in case of Cur-PLGA NPs and CH@Cur-PLGA C/SNPs, the characteristic peaks of Cur were absent indicating that Cur might be encapsulated in PLGA NPs and CH@PLGA C/SNPs [21].

XRD patterns of all samples viz. pure Cur, CH, PLGA, blank PLGA NPs, blank CH@PLGA C/SNPs, Cur-PLGA NPs and CH@Cur-PLGA C/SNPs were carried out to study the crystalline nature and depicted in Fig. 1B. Diffractogram of CH showed intense peak at 2θ values of 19.82, revealing high degree of crystallinity [24]. The diffractogram of pure Cur showed intense peaks at 2θ values of 7.90, 8.88, 12.20, 14.54 and 17.34 revealing the crystallinity of Cur [26]. However, PLGA did not show any sharp intense peak indicating its amorphous nature [27]. The diffractograms of lyophilized powder of blank PLGA NPs, blank CH@PLGA C/SNPs, Cur-PLGA NPs and CH@Cur-PLGA C/SNPs demonstrated diminished characteristic peaks of Cur as compared to pure Cur, which revealed that crystalline nature of Cur has decreased and has been dispersed molecularly in the PLGA matrix. However, the intense peak at 2θ values of 19.18 and 23.34, in lyophilized blank PLGA NPs, blank CH@PLGA C/SNPs, Cur-PLGA NPs and CH@Cur-PLGA C/SNPs were the characteristic peaks of mannitol [28].

The TEM images of Cur-PLGA NPs and CH@Cur-PLGA C/SNPs demonstrated smooth surface with spherical shape along with uniform size distribution in the range of 175–225 nm, which are depicted in Fig. 1C and D. The significance of smooth and spherical shape is that it has lesser plasma protein adsorption and later opsonisation and is poor entity for RES and liver uptake [29]. The CH as shell was coated over the PLGA NPs uniformly, resulting into formation of CH@Cur-PLGA C/SNPs as demonstrated in Fig. 1D. The obtained size of Cur-PLGA NPs and CH@Cur-PLGA C/SNPs obtained from TEM resembles the data of particle size obtained by particle size analyser.

3.3. In-vitro release study

In-vitro release of Cur from Cur suspension, Cur-PLGA NPs and CH@Cur-PLGA C/S NPs was performed to investigate sustain release of Cur as well as discover the effect of CH coating (shell) on Cur release form PLGA NPs. The results are depicted in Fig. 2A. The results demonstrated that Cur suspension released 91.4 ± 1.5% of Cur after 12 h, revealing immediate release of Cur. However, Cur release from CUR-PLGA NPs demonstrated biphasic release behaviour that is initially burst release was obtained followed by sustained release i.e. 81.96 ± 1.33% after 96 h. The initial burst release of Cur might be due to the adsorption of Cur on the surface of PLGA NPs as well as Cur solubility in the dissolution medium [30]. As compared to Cur-PLGA NPs, Cur release from CH@Cur-PLGA C/S NPs demonstrated slow and sturdy release at each time point. The results revealed that Cur release from CH@Cur-PLGA C/S NPs was found to be of 66.73 ± 1.28% after 96 h. There was no burst release from CH@Cur-PLGA C/S NPs revealing coating of CH over the surface of PLGA NPs which acts as a barrier for PLGA NPs limiting its diffusion/erosion process of Cur from PLGA NPs [6].

3.4. Ex-vivo diffusion study

Ex-vivo diffusion of Cur from Cur-PLGA NPs and CH@Cur-PLGA C/S NPs was performed using franz-diffusion cell involving goat nasal mucosa. The results indicated that after 24 h, Cur from Cur suspension was diffused up to 39.59 ± 1.38%. However, Cur from Cur-PLGA NPs and CH@Cur-PLGA C/S NPs was showed 61.24 ± 1.31% and 79.28 ± 1.37% of release after 24 h. The CH@Cur-PLGA C/S NPs exhibited higher amount of Cur diffusion through nasal mucosa was owing to the presence of cationic CH over the surface of PLGA NPs which act as a permeation enhancer [30]. Additionally, CH also has the ability to open tight junctions of nasal mucosa. CH positive charge interacted with anionic group of nasal membrane is also involved in permeation enhancement of CH@Cur-PLGA C/SNPs [6].

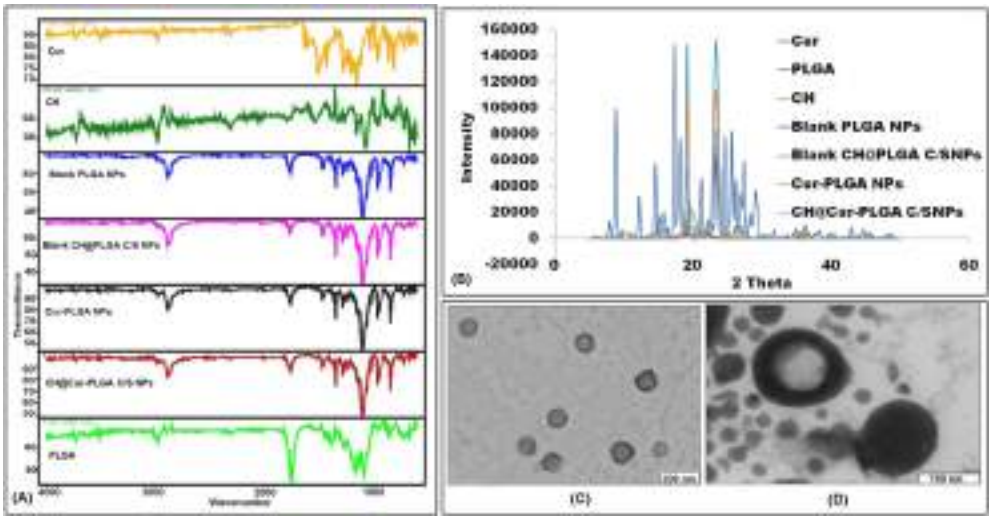

Fig. 1. Characterization of pure Cur, Cur-PLGA NPs and CH@Cur-PLGA C/SNPs by FTIR (A); pXRD (B); and TEM of Cur-PLGA NPs (C); TEM of CH@Cur-PLGA C/SNPs (D).

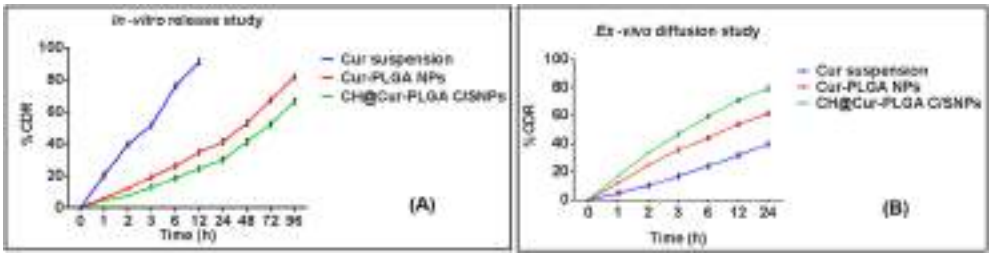

Fig. 2. *In-vitro* release study (A) and *Ex-vivo* permeation study (B) of pure Cur, Cur-PLGA NPs and CH@Cur-PLGA C/SNPs.

3.5. In-vitro cell viability assay

The NPs when administered intranasally, exposed to two distinct tissues viz. nasal cavity and brain tissue. Thus need to investigate the NPs-based cytotoxicity to either of them. Therefore, in order to investigate RPMI 2650 (human nasal cells) and SH-SY-5Y (human neuroblastoma) cell lines were considered for biocompatibility and safety of prepared NPs. The results (Fig. 3A and B) demonstrated that prepared NPs viz. blank PLGA NPs, blank CH@PLGA C/S NPs, Cur-PLGA NPs and CH@Cur-PLGA C/S NPs along with pure Cur with distinct concentrations of 0, 10, 20, 30, 40 and 50 μg/ml, when exposed to both the cell lines individually for 24 h; there was no cytotoxicity occurred and showed greater cell-viability in both cell lines. The % cell viability of all the samples was found to be greater than 90% after 24 h of exposure. As CH and PLGA has been approved by FDA as GRAS category and Cur being flavonoid, we can suggest that developed nanoparticles are biocompatible and do not cause cell cytotoxicity till 50 μg/ml of concentration.

3.6. Cellular uptake of prepared NPs

Cellular uptake of FITC (as control), blank FITC-PLGA NPs, blank FITC-CH@PLGA C/S NPs, FITC-Cur-PLGA NPs and FITC-CH@Cur-PLGA C/S NPs were quantitatively evaluated by spectrofluorometer in SH-SY-5Y cell line. The results (Fig. 4A) demonstrated that fluorescence intensity of FITC conjugated NPs was much higher inside the cell than that of control group (FITC). However, CH@Cur-PLGA C/SNPs exhibited higher fluorescence intensity as compared to other NPs. The results showed that FITC showed very less cellular uptake (1.7%) as compared to cellular uptake of blank FITC-PLGA NPs, blank FITC-CH@PLGA C/S NPs, FITC-Cur-PLGA NPs and FITC-CH@Cur-PLGA C/S NPs 39.6 ± 3.9%, 38.1 ± 4.1%, 40.5 ± 5.7% and 55.4 ± 3.8%, respectively. The aforementioned results demonstrated that coating of shell (CH) may significantly affect cellular uptake of NPs as positive charge of CH@Cur-PLGA C/S NPs has the ability to interact electrostatically with negative charge of cell membrane, as compared to neutral and negatively charged NPs [31]. Therefore, the investigation revealed that cellular uptake of Cur was enhanced owing to the presence of CH (shell) over the surface of PLGA NPs, when administered intranasally.

3.7. Cellular uptake mechanism study

In order to investigate type of endocytic pathway involved in transport of prepared NPs, the cellular uptake mechanism study was performed using several endocytic pathway inhibitors viz. sodium azide, nystatin and chlorpromazine inhibiting macropinocytosis, caveolae-mediated and clathrin-mediated pathway using SH-SY-5Y cell line and analysed by spectrofluorometer (Fig. 4B). The reduction in cellular uptake of blank PLGA NPs, blank CH@PLGA C/S NPs, Cur-PLGA NPs and CH@Cur-PLGA C/S NPs was found to be 25.25 ± 3.20%, 14.96 ± 3.10%, 22.22 ± 5.10%, 26.36 ± 3.60%, respectively (% reduction in internalization) when sodium azide was exposed to SH-SY-5Y cells. The results revealed that macropinocytosis pathway was lesser utilized by prepared NPs. The hydrophilic and cationic nature of C/S NPs may be responsible for escaping macropinocytosis [17]. The reduction in cellular uptake of blank PLGA NPs, blank CH@PLGA C/S NPs, Cur-PLGA NPs and CH@Cur-PLGA C/S NPs was found to be 19.95 ± 4.10%, 20.73 ± 4.30%, 24.20 ± 5.10%, 22.56 ± 4.40%, respectively when chlorpromazine was exposed to SH-SY-5Y cells. The previous studies demonstrated that clathrin-mediated pathway usually followed by NPs having particle size less than 200 nm for cellular uptake [32]. The reduction in cellular uptake of blank PLGA NPs, blank CH@PLGA C/S NPs, Cur-PLGA NPs and CH@Cur-PLGA C/S NPs was found to be 37.63 ± 4.90%, 32.81 ± 4.40%, 30.62 ± 3.30%, 51.44 ± 5.40%, respectively when nyststin was exposed to SH-SY-5Y cells. The results demonstrated that amongst all three pathways, the internalization of prepared NPs were much higher by caveolae-mediated endocytosis-based pathway as compared to clathrin-mediated pathway and macropinocytosis [33,34].

3.8. ROS generation study

In order to investigate whether prepared NPs viz. blank PLGA NPs, blank CH@PLGA C/S NPs, Cur-PLGA NPs and CH@Cur-PLGA C/S NPs along with pure Cur are responsible for generating ROS or not, the study was performed using RAW 264.7 cell line. All the samples with distinct concentrations viz. 10, 20, 30, 40 and 50 μg/ml were exposed, whereas control group indicates the cells with no treatment of NPs. The results (Fig. 5A) demonstrated that control group exhibited the relative fluorescent intensity of 9.2 ± 2.9%. Similarly, when pure Cur, blank PLGA NPs, blank CH@PLGA C/SNPs, Cur-PLGA NPs and CH@Cur-PLGA C/SNPs were exposed to RAW 264.7 cells, they exhibited insignificant

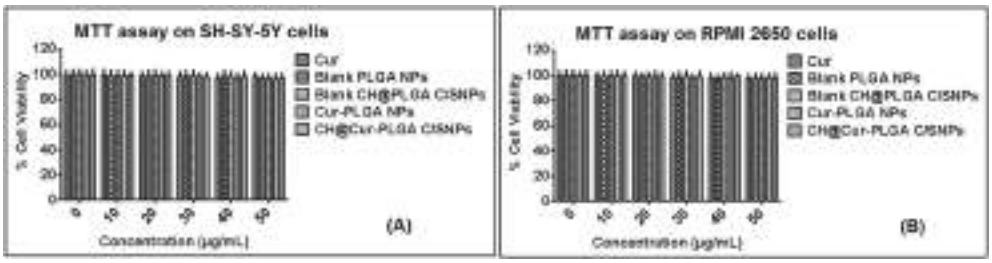

Fig. 3. *In-vitro* cell line studies of pure Cur, blank PLGA NPs, blank CH@PLGA C/SNPs, Cur-PLGA NPs and CH@Cur-PLGA C/SNPs: MTT assay on SH-SY-5Y cell line (A) and RPMI 2650 cell line (B).

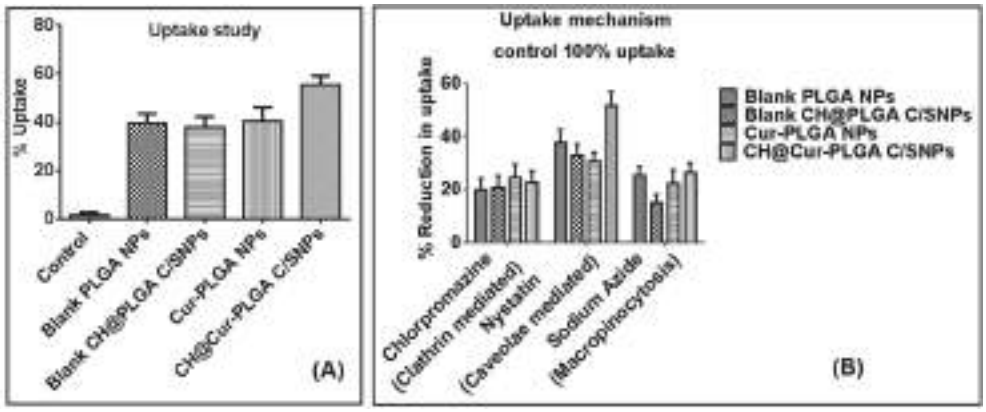

Fig. 4. Quantitative cellular uptake of Cur-PLGA NPs and CH@Cur-PLGA C/SNPs (A); Cellular uptake mechanism of blank PLGA NPs, blank CH@PLGA C/SNPs, Cur-PLGA NPs and CH@Cur-PLGA C/SNPs (B).

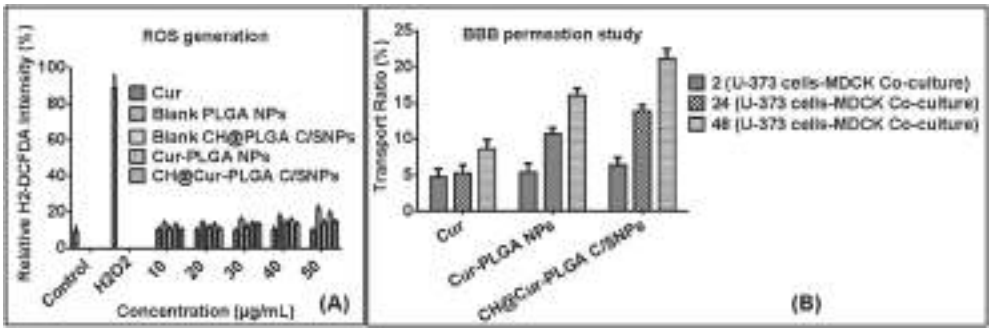

Fig. 5. ROS generation on RAW 264.7 cell line (A); BBB permeation study using co-culture model (MDCK II and U 373 MG cells) (B); of blank PLGA NPs, blank CH@PLGA C/S NPs, Cur-PLGA NPs and CH@Cur-PLGA C/S NPs.

change in the relative fluorescent intensity in the cells. Briefly, pure Cur, blank PLGA NPs, blank CH@PLGA C/SNPs, Cur-PLGA NPs and CH@Cur-PLGA C/SNPs at a concentration of 50 µg/ml exhibited relative fluorescent intensity of 9.80 ± 1.1%, 21.4 ± 2.3%, 13.5 ± 2.1%, 18.6 ± 2.1% and 14.5 ± 1.3%, respectively, which is insignificant when compared to control and far lesser than H_2O_2 (88.7 ± 7.4%) exposed group. Thus, in a conclusion, the ROS generation study demonstrated that pure Cur, blank PLGA NPs, blank CH@PLGA C/SNPs, Cur-PLGA NPs and CH@Cur-PLGA C/SNPs, till the concentration of 50 µg/ml was not generating ROS, suggesting that till this concentration, these formulations are safe, as increase in ROS generation leads to decrease in cell viability. Therefore, aforementioned concentration of Cur-PLGA NPs and CH@Cur-PLGA C/SNPs can be employed in AD for antioxidant activity.

3.9. In-vitro BBB permeation study

As reported previously that nasal cavity consist of rich vasculature, thus NPs administered intranasally, have the possibility of entering blood circulation. Thus, to study the ability of NPs to permeate BBB which enter the blood circulation through nasal cavity, in-vitro BBB permeation study was performed using co-culture model of BBB consisting of MDCK II cells and U 373 MG cells. The results (Fig. 5B) indicated that transport ratio of pure CUR was lesser when compared with Cur-PLGA NPs and CH@Cur-PLGA C/S NPs. The results also revealed that cellular uptake of NPs were dependent on time. In brief, the transport ratio of pure Cur, Cur-PLGA NPs and CH@Cur-PLGA C/S NPs through BBB was found to be 4.7 ± 1.2%, 5.4 ± 1.2% and 6.4 ± 1.1%, respectively after 2 h of exposure. However, the transport ratio of pure Cur, Cur-PLGA NPs and CH@Cur-PLGA C/S NPs through BBB was found to be 5.3 ± 1.1%, 10.7 ± 0.9% and 13.9 ± 0.8%, respectively after 24 h of exposure. The transport ratio of pure Cur, Cur-PLGA NPs and CH@Cur-PLGA C/S NPs through BBB was found to be 8.6 ± 1.3%, 16.1 ± 0.9% and 21.2 ± 1.3%, respectively after 48 h of exposure. Thus, from in-vitro BBB permeation study it can said that Cur when loaded in NPs more specifically C/SNPs exhibited more permeation as compared to pure Cur.

3.10. Antioxidant assay

The antioxidant activity of pure CUR and fabricated NPs viz. Cur-PLGA NPs and CH@Cur-PLGA C/S NPs was investigated using three different assays MDA, CAT and SOD. The MDA assay (Fig. 6) results indicated that as compared to positive control group, the various concentrations of pure Cur, Cur-PLGA NPs and CH@Cur-PLGA C/S NPs were able to significantly reduce MDA level. Whereas, as compared to negative control, MDA level was significantly increased in positive control group [18,35]. Correspondingly, various concentrations of pure Cur, Cur-PLGA NPs and CH@Cur-PLGA C/S NPs showed significant increase in CAT activity as compared to negative and positive control (Fig. 7). Further, SOD assay results (Fig. 8) showed that lower concentration of pure Cur indicated increase in SOD activity as compared to control when cells were exposed to H_2O_2 for 8 h. However, as compared to negative control group, the higher concentration (20 mM) of pure Cur showed significant reduction in SOD activity. Similarly, as compared to positive control group, at lower concentration (5 mM) of Cur-PLGA NPs and CH@Cur-PLGA C/SNPs showed significant increase in SOD activity when cells were exposed to H_2O_2 for 8 h. However, at higher concentration (10 mM and 20 mM) of Cur-PLGA NPs and CH@Cur-PLGA C/SNPs led to significant reduction in SOD activity as compared to negative control group. SOD catalyzes the O_2- (superoxide) radical to form either H_2O_2 or ordinary molecular oxygen (O_2). The overall results

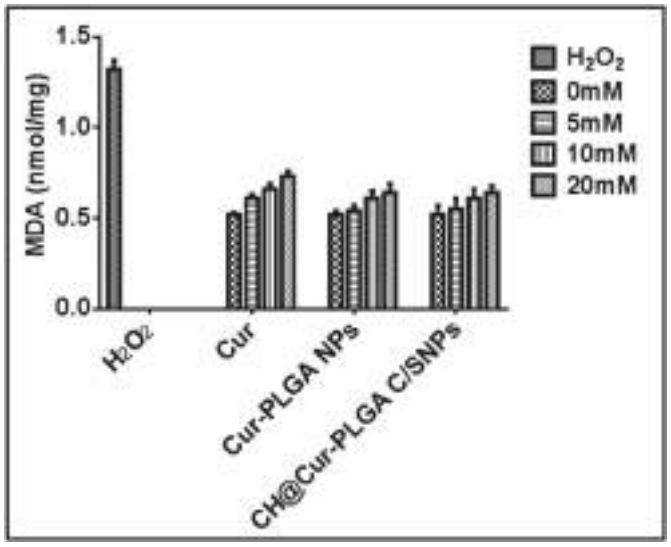

Fig. 6. Antioxidant assay using MDA level of pure Cur, Cur-PLGA NPs and CH@Cur-PLGA C/SNPs.

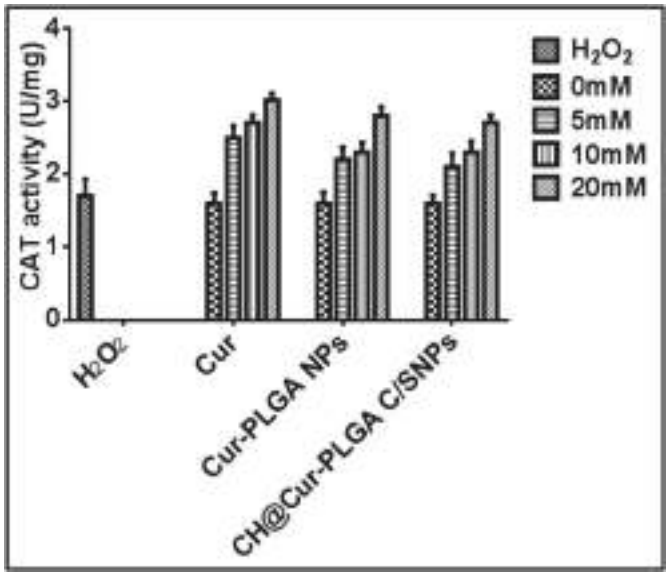

Fig. 7. Antioxidant assay using CAT activity MDA level of pure Cur, Cur-PLGA NPs and CH@Cur-PLGA C/SNPs.

demonstrated that lower concentration of pure Cur, Cur-PLGA NPs and CH@Cur-PLGA C/SNPs exhibited significant effect on ROS scavenging. However, higher dose of pure Cur, Cur-PLGA NPs and CH@Cur-PLGA C/SNPs can induce the ROS generation.

3.11. Biodistribution study

The biodistribution of FITC-Cur-PLGA NPs and FITC-CH@Cur-PLGA C/SNPs was determined using obtained calibration curve in various organs. The results of biodistribution study were expressed as percentage dose per gram of tissue (% total dose/g) to compensate for possible variation between animals and are depicted in Fig. 9. The results demonstrated that after 12 h of intranasal administration, the amount of Cur in various organs such as liver, kidney, lungs, brain, heart and spleen was found to be 0.13 ± 0.04%, 0.24 ± 0.09%, 0.18 ± 0.05%, 0.11 ± 0.03%, 0.13 ± 0.04% and 0.52 ± 0.04%, respectively. Whereas, the amount of CUR in liver, kidney, lungs, brain, heart and spleen was found

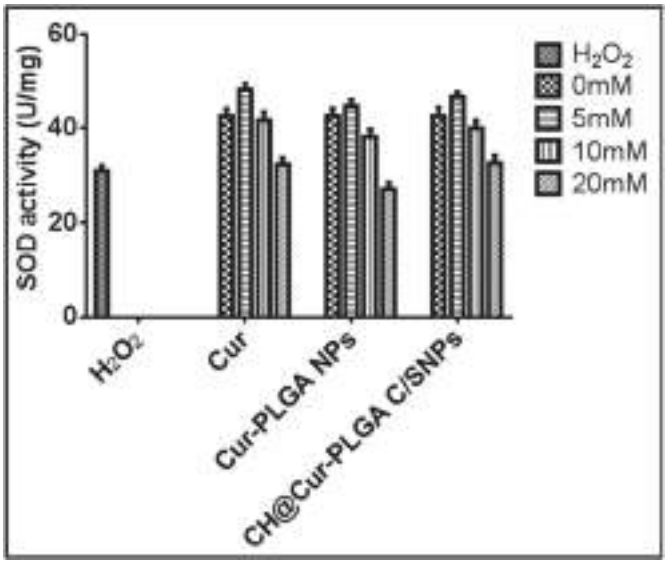

Fig. 8. Antioxidant assay using SOD activity of pure Cur, Cur-PLGA NPs and CH@Cur-PLGA C/SNPs.

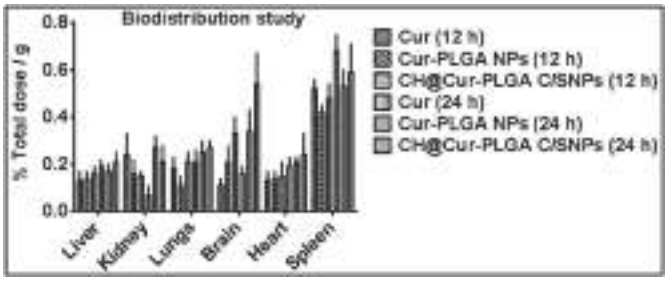

Fig. 9. Bio-distribution study of pure Cur, Cur-PLGA NPs and CH@Cur-PLGA C/SNPs.

to be 0.19 ± 0.03%, 0.27 ± 0.04%, 0.21 ± 0.05%, 0.16 ± 0.03%, 0.19 ± 0.04%, 0.68 ± 0.07%, respectively, after 24 h of intranasal administration. However, after 12 h of intranasal administration the amount of FITC-Cur-PLGA NPs in various organs like liver, kidney, lungs, brain, heart and spleen was found to be 0.14 ± 0.03%, 0.16 ± 0.06%, 0.11 ± 0.04%, 0.21 ± 0.07%, 0.14 ± 0.03% and 0.42 ± 0.03%, respectively. Whereas, the amount of FITC-Cur-PLGA NPs in various organs viz. liver, kidney, lungs, brain, heart and spleen was found to be 0.17 ± 0.03%, 0.27 ± 0.05%, 0.25 ± 0.05%, 0.34 ± 0.09%, 0.21 ± 0.02% and 0.53 ± 0.07%, respectively, after 24 h of intranasal administration. Moreover, after 12 h of intranasal administration the amount of FITC-CH@Cur-PLGA C/SNPs in various organs like liver, kidney, lungs, brain, heart and spleen was found to be 0.16 ± 0.03%, 0.15 ± 0.02%, 0.21 ± 0.04%, 0.33 ± 0.07%, 0.15 ± 0.06% and 0.48 ± 0.06%, respectively. Whereas, the amount of FITC-CH@Cur-PLGA C/SNPs in various organs viz. liver, kidney, lungs, brain, heart and spleen was found to be 0.21 ± 0.04%, 0.21 ± 0.07%, 0.27 ± 0.03%, 0.54 ± 0.13%, 0.24 ± 0.09% and 0.59 ± 0.12%, respectively, after 24 h of intranasal administration. The results suggested that as compared to 12 h, the biodistribution of FITC-Cur-PLGA NPs and FITC-CH@Cur-PLGA C/SNPs was higher in each organ after 24 h of intranasal administration. Nonetheless, as compared to Cur-PLGA NPs, the amount of CH@Cur-PLGA C/SNPs was found higher in brain, indicating that CH-based surface modification of PLGA NPs can enhance targeting efficiency to the brain. Additionally, highest amount of Cur, FITC-Cur-PLGA NPs and FITC- CH@Cur-PLGA C/SNPs in spleen can be explained by fact that when Cur, FITC-Cur-PLGA NPs and FITC-CH@Cur-PLGA C/SNPs entered the systemic circulation interacts with

coagulation factors, blood cells and plasma proteins and these interacted product recognized by residential macrophages and removed by the spleen [36]. Additionally, the results also revealed that CH@Cur-PLGA C/SNPs can efficiently transport the Cur to the brain using intranasal route.

3.12. In vivo toxicity study

As previously reported that NPs administered through nasal route can enter systemic circulation due to the presence of rich vasculature in nasal cavity; therefore need to study the systemic toxicity of administered NPs. The study was performed by assessing biochemical parameters of blood after intranasal administration in mice. The results indicated that there were no signs or symptoms of change in behaviour or movement or any toxicity during or post-treatment of 7 days. Additionally, no mortality or toxicity related clinical signs were observed in mice after consecutive dosing for 7 days (Table 1). The results showed that examination of blood with respect to NPs administered groups showed insignificant effect on haematological and biochemical parameter values as compared to control group [20]. Thus, it can be concluded that both Cur-PLGA NPs and CH@Cur-PLGA C/SNPs were safe to be administered via intranasal route.

3.13. Stability studies

3.13.1. Photostability study

The photostability of Cur is necessary as in presence of light Cur leads to degradation and lowers the therapeutic efficacy therefore; stability of Cur is matter of concern in pharmaceutical and food industries. Secondly, the study was performed to investigate the ability of prepared NPs to protect Cur from photodegradation. Thus, photostability study was performed to compare stability of Cur in Cur suspension and when incorporated in PLGA NPs and CH@PLGA C/SNPs. The results (Fig. 10) indicated that Cur stability in PLGA NPs and CH@PLGA C/S NPs when exposed to UV was found to be 74.37 ± 1.51% and 81.70 ± 1.13% (% Cur retention) which was far greater than that of Cur in Cur suspension i.e. 3.19 ± 1.50% after 24 h. The results suggest that Cur is protected by PLGA NPs and CH@PLGA C/SNPs from external environmental factors. However, CH@Cur-PLGA C/SNPs were capable of retaining more amount Cur as compared to Cur-PLGA NPs which may due to coating of CH shell over PLGA NPs.

3.13.2. Thermal stability study

Similar to photostability of Cur, it's necessary to investigate thermal stability of Cur and to investigate ability of prepared NPs to protect Cur from thermal degradation. Thermal stability [22] of Cur-PLGA NPs and CH@Cur-PLGA C/SNPs was performed at 4 °C, 25 °C and 30 °C for 30 days by assessing particle size, polydispersivity and zeta potential against pure Cur suspension. The results showed that both type of NPs were found to be stable when stored at 4 °C, 25 °C and 30 °C. However, it was found that as the temperature increased the average particle size of NPs, polydispersivity was increased and surface charge was decreased but was not significant. The effect of temperature on particle size, polydispersivity and surface charge are demonstrated in Fig. 11A, B and 11C, respectively. The initial particle size, polydispersivity and zeta potential on Cur suspension at 4 °C, 25 °C and 30 °C was 648.40 ± 5.91 nm, 0.564 ± 0.027 and −25.1 ± 1.30 mV, respectively. However, at the end of 30 days, the particle size of Cur suspension when stored at 4 °C, 25 °C and 30 °C was found to be 1539.00 ± 4.93 nm, 1900 ± 7.75 nm and 2431.7 ± 5.19 nm, respectively, which revealed the instability of Cur in suspension form. At all the exposed temperature PDI showed high polydispersivity of suspension (PDI = 1.00) indicating high polydispersivity in suspension. Surface charge of Cur suspension at all exposed temperature was reduced from −25.1 ± 1.30 mV to low negative i.e. near to −9.00 ± 1.03 mV.

The initial particle size, polydispersivity and zeta potential of Cur-PLGA NPs at 4 °C, 25 °C and 30 °C was 193.2 ± 1.21 nm, 0.124 ± 0.015 and −29.80 ± 1.39 mV, respectively. However, at the end of 30 days, the particle size of Cur-PLGA NPs when stored at 4 °C, 25 °C and 30 °C was found to be 199.9 ± 2.47 nm, 203.2 ± 2.95 nm and 211.6 ± 2.89 nm, respectively, which revealed that as temperature increased the particle size of Cur-PLGA NPs were also increased. At all the exposed temperature, PDI and surface charge showed insignificant effect indicating colloidal solution of Cur-PLGA NPs were uniformly dispersed and stable. The initial particle size, polydispersivity and zeta potential of CH@Cur-PLGA C/SNPs at 4 °C, 25 °C and 30 °C was 207.6 ± 2.91 nm, 0.165 ± 0.071 and +31.9 ± 1.09 mV, respectively. However, at the end of 30 days, the particle size of CH@Cur-PLGA C/SNPs when stored at 4 °C, 25 °C and 30 °C was found to be 217.1 ± 2.39 nm, 219.0 ± 3.09 nm and 231.9 ± 3.27 nm, respectively, which revealed that as temperature increased the particle size of CH@Cur-PLGA C/SNPs were also increased. At all the exposed temperature, PDI and surface charge showed insignificant effect indicating colloidal solution of CH@Cur-PLGA C/SNPs were uniformly dispersed and stable. The results conclude that prepared Cur-PLGA NPs and CH@Cur-PLGA C/SNPs showed greater stability at 4 °C for a month than that of when stored at 25 °C and 30 °C.

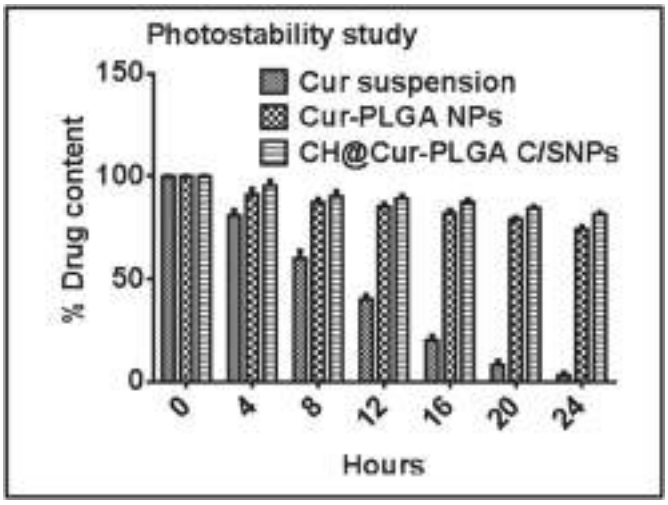

Fig. 10. Photostability study of pure Cur, Cur-PLGA NPs and CH@Cur-PLGA C/SNPs.

Table 1
In-vivo toxicity assessment by estimating biochemical parameters after intranasal administration of NPs (Cur-PLGA NPs and CH@Cur-PLGA C/SNPs) after 7 days.

Parameters	Control	Cur-PLGA NPs	CH@Cur-PLGA C/SNPs
HB%	13.06 ± 0.42	15.10 ± 0.50	14.96 ± 0.35
RBC *10^3/cmm	8.13 ± 0.81	8.27 ± 0.35	8.25 ± 0.47
WBC*10^3/cmm	8.15 ± 2.31	8.33 ± 0.61	8.19 ± 0.67
PLT*10^5/cmm	5.24 ± 0.47	5.11 ± 0.39	5.26 ± 0.43
N%	51.7 ± 3.15	54.06 ± 4.72	55.17 ± 4.94
E%	0.65 ± 0.07	0.69 ± 0.04	0.68 ± 0.05
L%	31.25 ± 2.81	33.57 ± 3.24	34.61 ± 3.57
M%	0.84 ± 0.04	0.89 ± 0.02	0.89 ± 0.04
PCV%	48.5 ± 5.02	48.39 ± 3.9	49.77 ± 5.9
Bil (mg/dl)	0.35 ± 0.03	0.38 ± 0.03	0.39 ± 0.05
OT (IU/L)	189.2 ± 21.75	193.6 ± 19.4	195.1 ± 25.2
PT (IU/L)	141 ± 24.3	149.6 ± 22.1	146.5 ± 19.7
ALK (IU/L)	132 ± 11.8	137.5 ± 20.4	139.2 ± 24.1
PRO (g/dl)	8.09 ± 1.07	8.13 ± 1.11	8.14 ± 1.37
ALB (g/dl)	3.15 ± 0.47	3.20 ± 0.31	3.22 ± 0.53
GLB (g/dl)	4.39 ± 0.37	4.36 ± 0.41	4.43 ± 0.51
BUN (mg/dl)	11.20 ± 1.31	12.22 ± 1.21	12.27 ± 1.87
CREAT (mg/dl)	1.27 ± 0.42	1.37 ± 0.41	1.39 ± 0.39

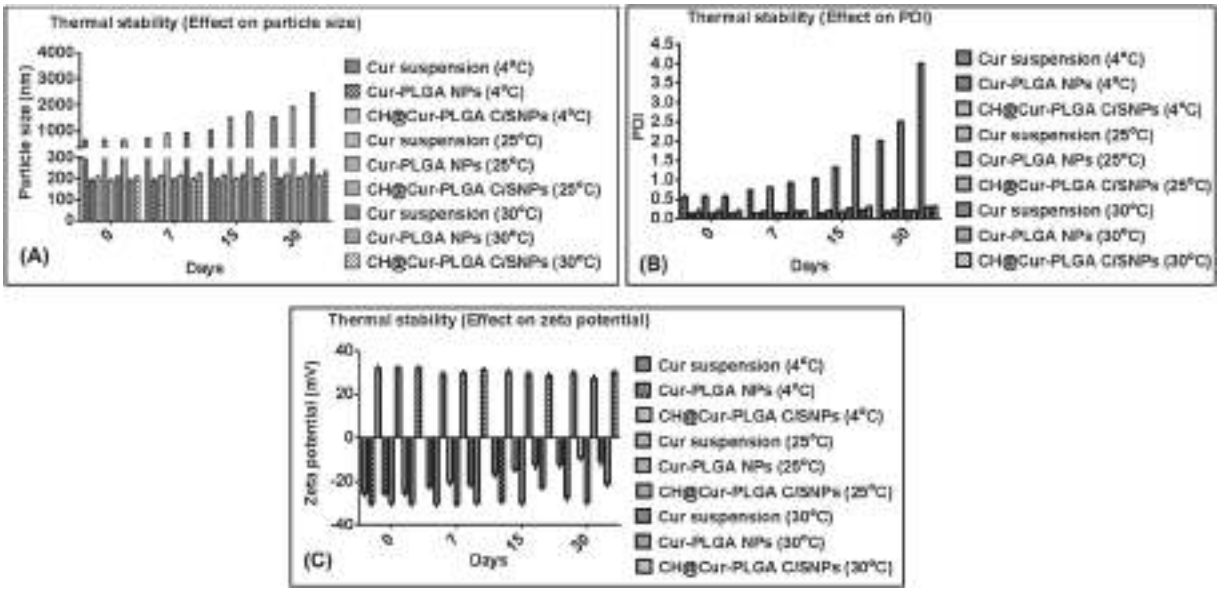

Fig. 11. Thermal stability study of pure Cur, Cur-PLGA NPs and CH@Cur-PLGA C/SNPs.

4. Conclusion

This investigation demonstrates that CH@Cur-PLGA C/S NPs were successfully fabricated, characterized and evaluated for intranasal delivery. Additionally, the effect of CH coating over PLGA NPs on release of Cur, permeation of NPs through nasal mucosa was performed demonstrating that owing to the presence of cationic CH, the Cur release was sustained and permeation of CH@Cur-PLGA C/S NPs was enhanced as compared to Cur-PLGA NPs. The NPs entering blood circulating after intranasal administration were efficiently permeated through BBB co-culture model, showing maximum amount of Cur distributed in brain. The systemic toxicity study confirmed that Cur-PLGA NPs and CH@Cur-PLGA C/S NPs were biocompatible and found to be safe. The antioxidant study revealed that Cur-PLGA NPs and CH@Cur-PLGA C/S NPs were able to efficiently attenuate oxidative stress occurring in AD. The overall results suggest Cur as potential remedy for attenuating oxidative stress while CH@Cur-PLGA C/SNPs as efficient carrier and intranasal route as an efficient route for of Cur in the treatment of AD.

CRediT authorship contribution statement

Namdev Dhas: Conceptualization, Methodology, Software, Data curation, Visualization, Investigation, Writing - original draft. **Tejal Mehta:** Conceptualization, Data curation, Supervision, Writing - review & editing.

Declaration of competing interest

The authors declare no conflict of interest.

Acknowledgement

Authors would like to thank Council of Scientific and Industrial Research (CSIR) and Institute of Pharmacy, Nirma University for providing financial assistance in the form of CSIR-Senior Research Fellowship (SRF) (09/1048(007)/2018-EMR-I) and Nirma University-Junior Research Fellowship (JRF) (NU/IP/stipend/Ph.D./2016) to Namdev Dhas. The authors are again thankful to Institute of Pharmacy, Nirma University for providing the necessary facilities to carry out the research work.

References

[1] N. Dhas, R. Kudarha, T. Mehta, Intranasal delivery of nanotherapeutics/nanobiotherapeutics for the treatment of Alzheimer's disease: a propitious approach, CRT. https://doi.org/10.1615/CritRevTherDrugCarrierSyst.2018026762, 2020.
[2] A. Mathew, T. Fukuda, Y. Nagaoka, T. Hasumura, H. Morimoto, Y. Yoshida, T. Maekawa, K. Venugopal, D.S. Kumar, Curcumin loaded-PLGA nanoparticles conjugated with Tet-1 Peptide for potential use in Alzheimer's disease, PloS One 7 (2012), e32616, https://doi.org/10.1371/journal.pone.0032616.
[3] V. Piazzini, E. Landucci, M. D'Ambrosio, L. Tiozzo Fasiolo, L. Cinci, G. Colombo, D. E. Pellegrini-Giampietro, A.R. Bilia, C. Luceri, M.C. Bergonzi, Chitosan coated human serum albumin nanoparticles: a promising strategy for nose-to-brain drug delivery, Int. J. Biol. Macromol. 129 (2019) 267–280, https://doi.org/10.1016/j.ijbiomac.2019.02.005.
[4] N.L. Dhas, N.J. Raval, R.R. Kudarha, N.S. Acharya, S.R. Acharya, Chapter 9 - core–shell nanoparticles as a drug delivery platform for tumor targeting, in: A. M. Grumezescu (Ed.), Inorganic Frameworks as Smart Nanomedicines, William Andrew Publishing, 2018, pp. 387–448, https://doi.org/10.1016/B978-0-12-813661-4.00009-2.
[5] B. Shah, D. Khunt, M. Misra, H. Padh, Application of Box-Behnken design for optimization and development of quetiapine fumarate loaded chitosan nanoparticles for brain delivery via intranasal route*, Int. J. Biol. Macromol. 89 (2016) 206–218, https://doi.org/10.1016/j.ijbiomac.2016.04.076.
[6] N. Khan, null Ameeduzzafar, K. Khanna, A. Bhatnagar, F.J. Ahmad, A. Ali, Chitosan coated PLGA nanoparticles amplify the ocular hypotensive effect of forskolin: statistical design, characterization and in vivo studies, Int. J. Biol. Macromol. 116 (2018) 648–663, https://doi.org/10.1016/j.ijbiomac.2018.04.122.
[7] T.A. Mehta, N. Shah, K. Parekh, N. Dhas, J.K. Patel, Surface-modified PLGA nanoparticles for targeted drug delivery to neurons, in: Y.V. Pathak (Ed.), Surface Modification of Nanoparticles for Targeted Drug Delivery, Springer International Publishing, Cham, 2019, pp. 33–71, https://doi.org/10.1007/978-3-030-06115-9_3.
[8] M.A. Islam, T.-E. Park, E. Reesor, K. Cherukula, A. Hasan, J. Firdous, B. Singh, S.-K. Kang, Y.-J. Choi, I.-K. Park, C.-S. Cho, Mucoadhesive chitosan derivatives as novel drug carriers, Curr. Pharmaceut. Des. 21 (2015) 4285–4309, https://doi.org/10.2174/1381612821666150901103819.
[9] A. Abruzzo, T. Cerchiara, F. Bigucci, G. Zuccheri, C. Cavallari, B. Saladini, B. Luppi, Cromolyn-crosslinked chitosan nanoparticles for the treatment of allergic rhinitis, Eur. J. Pharmaceut. Sci. 131 (2019) 136–145, https://doi.org/10.1016/j.ejps.2019.02.015.
[10] N.L. Dhas, P.P. Ige, R.R. Kudarha, Design, optimization and in-vitro study of folic acid conjugated-chitosan functionalized PLGA nanoparticle for delivery of bicalutamide in prostate cancer, Powder Technol. 283 (2015) 234–245, https://doi.org/10.1016/j.powtec.2015.04.053.
[11] K. Sawant, A. Pandey, S. Patel, Aripiprazole loaded poly(caprolactone) nanoparticles: optimization and in vivo pharmacokinetics, Mater. Sci. Eng. C 66 (2016) 230–243, https://doi.org/10.1016/j.msec.2016.04.089.
[12] V. Venkateswarlu, K. Manjunath, Preparation, characterization and in vitro release kinetics of clozapine solid lipid nanoparticles, J. Contr. Release 95 (2004) 627–638, https://doi.org/10.1016/j.jconrel.2004.01.005.
[13] K. Jain, S. Sood, K. Gowthamarajan, Optimization of artemether-loaded NLC for intranasal delivery using central composite design, Drug Deliv. 22 (2015) 940–954, https://doi.org/10.3109/10717544.2014.885999.

[14] S. Tang, A. Wang, X. Yan, L. Chu, X. Yang, Y. Song, K. Sun, X. Yu, R. Liu, Z. Wu, P. Xue, Brain-targeted intranasal delivery of dopamine with borneol and lactoferrin co-modified nanoparticles for treating Parkinson's disease, Drug Deliv. 26 (2019) 700–707, https://doi.org/10.1080/10717544.2019.1636420.
[15] Q. Meng, A. Wang, H. Hua, Y. Jiang, Y. Wang, H. Mu, Z. Wu, K. Sun, Intranasal delivery of Huperzine A to the brain using lactoferrin-conjugated N-trimethylated chitosan surface-modified PLGA nanoparticles for treatment of Alzheimer's disease, Int. J. Nanomed. 13 (2018) 705–718, https://doi.org/10.2147/IJN.S151474.
[16] A. Pandey, K. Singh, S. Patel, R. Singh, K. Patel, K. Sawant, Hyaluronic acid tethered pH-responsive alloy-drug nanoconjugates for multimodal therapy of glioblastoma: an intranasal route approach, Mater. Sci. Eng. C 98 (2019) 419–436, https://doi.org/10.1016/j.msec.2018.12.139.
[17] G.D. Paka, C. Ramassamy, Optimization of curcumin-loaded PEG-PLGA nanoparticles by GSH functionalization: investigation of the internalization pathway in neuronal cells, Mol. Pharm. 14 (2017) 93–106, https://doi.org/10.1021/acs.molpharmaceut.6b00738.
[18] X. Lin, D. Bai, Z. Wei, Y. Zhang, Y. Huang, H. Deng, X. Huang, Curcumin attenuates oxidative stress in RAW264.7 cells by increasing the activity of antioxidant enzymes and activating the Nrf2-Keap1 pathway, PloS One 14 (2019), e0216711, https://doi.org/10.1371/journal.pone.0216711.
[19] S.M. Navarro, C. Darensbourg, L. Cross, R. Stout, D. Coulon, C.E. Astete, T. Morgan, C.M. Sabliov, Biodistribution of PLGA and PLGA/chitosan nanoparticles after repeat-dose oral delivery in F344 rats for 7 days, Ther. Deliv. 5 (2014) 1191–1201, https://doi.org/10.4155/tde.14.79.
[20] A. Pandey, K. Singh, S. Subramanian, A. Korde, R. Singh, K. Sawant, Heterogeneous surface architectured pH responsive Metal-Drug Nano-conjugates for mitochondria targeted therapy of Glioblastomas: a multimodal intranasal approach, Chem. Eng. J. 394 (2020) 124419, https://doi.org/10.1016/j.cej.2020.124419.
[21] A. Ranganathan, Y. Manabe, T. Sugawara, T. Hirata, N. Shivanna, V. Baskaran, Poly (D, L-lactide-co-glycolide)-phospholipid nanocarrier for efficient delivery of macular pigment lutein: absorption pharmacokinetics in mice and antiproliferative effect in Hep G2 cells, Drug Deliv Transl Res 9 (2019) 178–191, https://doi.org/10.1007/s13346-018-0590-9.
[22] C. Chittasupho, P. Posritong, P. Ariyawong, Stability, cytotoxicity, and retinal pigment epithelial cell binding of hyaluronic acid-coated PLGA nanoparticles encapsulating lutein, AAPS PharmSciTech 20 (2018) 4, https://doi.org/10.1208/s12249-018-1256-0.
[23] B. Lu, X. Lv, Y. Le, Chitosan-modified PLGA nanoparticles for control-released drug delivery, Polymers 11 (2019), https://doi.org/10.3390/polym11020304.
[24] A.Shak Tzeyung, S. Md, S.K. Bhattamisra, T. Madheswaran, N.A. Alhakamy, H. M. Aldawsari, A.K. Radhakrishnan, Fabrication, optimization, and evaluation of rotigotine-loaded chitosan nanoparticles for nose-to-brain delivery, Pharmaceutics 11 (2019), https://doi.org/10.3390/pharmaceutics11010026.
[25] P. Udompornmongkol, B.-H. Chiang, Curcumin-loaded polymeric nanoparticles for enhanced anti-colorectal cancer applications: J. Biomater. Appl. (2015) https://doi.org/10.1177/0885328215594479.
[26] G. Arya, M. Das, S.K. Sahoo, Evaluation of curcumin loaded chitosan/PEG blended PLGA nanoparticles for effective treatment of pancreatic cancer, Biomed. Pharmacother. 102 (2018) 555–566, https://doi.org/10.1016/j.biopha.2018.03.101.
[27] D. Deepika, H.K. Dewangan, L. Maurya, S. Singh, Intranasal drug delivery of frovatriptan succinate-loaded polymeric nanoparticles for brain targeting, J Pharm Sci 108 (2019) 851–859, https://doi.org/10.1016/j.xphs.2018.07.013.
[28] P. Mathur, S. Sharma, S. Rawal, B. Patel, M.M. Patel, Fabrication, optimization, and in vitro evaluation of docetaxel-loaded nanostructured lipid carriers for improved anticancer activity, J. Liposome Res. (2019) 1–15, https://doi.org/10.1080/08982104.2019.1614055.
[29] D.S. Jain, A.N. Bajaj, R.B. Athawale, S.S. Shikhande, A. Pandey, P.N. Goel, R. P. Gude, S. Patil, P. Raut, Thermosensitive PLA based nanodispersion for targeting brain tumor via intranasal route, Mater. Sci. Eng. C 63 (2016) 411–421, https://doi.org/10.1016/j.msec.2016.03.015.
[30] N. Ahmad, R. Ahmad, R.A. Alrasheed, H.M.A. Almatar, A.S. Al-Ramadan, M. Amir, M. Sarafroz, Quantification and evaluations of catechin hydrate polymeric nanoparticles used in brain targeting for the treatment of epilepsy, Pharmaceutics 12 (2020), https://doi.org/10.3390/pharmaceutics12030203.
[31] E.C. Cho, J. Xie, P.A. Wurm, Y. Xia, Understanding the role of surface charges in cellular adsorption versus internalization by selectively removing gold nanoparticles on the cell surface with a I2/KI etchant, Nano Lett. 9 (2009) 1080–1084, https://doi.org/10.1021/nl803487r.
[32] H. Hillaireau, P. Couvreur, Nanocarriers' entry into the cell: relevance to drug delivery, Cell. Mol. Life Sci. 66 (2009) 2873–2896, https://doi.org/10.1007/s00018-009-0053-z.
[33] S.D. Conner, S.L. Schmid, Regulated portals of entry into the cell, Nature 422 (2003) 37–44, https://doi.org/10.1038/nature01451.
[34] J. Rejman, V. Oberle, I.S. Zuhorn, D. Hoekstra, Size-dependent internalization of particles via the pathways of clathrin- and caveolae-mediated endocytosis, Biochem. J. 377 (2004) 159–169, https://doi.org/10.1042/BJ20031253.
[35] A. Daverey, S.K. Agrawal, Pre and post treatment with curcumin and resveratrol protects astrocytes after oxidative stress, Brain Res. 1692 (2018) 45–55, https://doi.org/10.1016/j.brainres.2018.05.001.
[36] W.I. Hagens, A.G. Oomen, W.H. de Jong, F.R. Cassee, A.J.A.M. Sips, What do we (need to) know about the kinetic properties of nanoparticles in the body? Regul. Toxicol. Pharmacol. 49 (2007) 217–229, https://doi.org/10.1016/j.yrtph.2007.07.006.